Probing transient photoinduced charge-transfer in Prussian Blue Analogues with time-resolved XANES and optical spectroscopy

S. Zerdane, Marco Cammarata, Lodovico Balducci, Roman Bertoni, Laure Catala, Sandra Mazerat, Talal Mallah, Martin N Pedersen, Michael Wulff, Kosuke N Nakagawa, et al.

Probing transient photoinduced charge-transfer in Prussian Blue Analogues with time-resolved XANES and optical spectroscopy

Serhane Zerdane,[a] Marco Cammarata,*[a] Lodovico Balducci,[a] Roman Bertoni,[a] Laure Catala,[b] Sandra Mazerat, [b] Talal Mallah, [b] Martin N. Pedersen,[c] Michael Wulff,[c] Kosuke Nakagawa,[d] Hiroko Tokoro,[e] Shin-ichi Ohkoshi,[d] Eric Collet,*[a]

Abstract: We study the transient electron transfer process in CsCoFe and RbMnFe Prussian Blue Analogues (PBA), by time-resolved X-ray Absorption Near Edge Structure (XANES) and by time-resolved optical spectroscopy. We performed time-resolved studies on CsCoFe nanocrystals dispersed in solution. The XANES results obtained at room temperature clearly evidence the $Co^{III}(LS)Fe^{II} \rightarrow Co^{II}(HS)Fe^{III}$ electron transfer between the metal centers, through the opposite spectral shifts at the Fe and Co edges. We also studied the $Mn^{III}(LS)Fe^{II} \rightarrow Mn^{II}(HS)Fe^{III}$ process in RbMnFe powder sample, at thermal equilibrium as well and under laser excitation. Optical spectroscopy reveals that the process occurs on the picosecond timescale, as already reported by Raman spectroscopy and that the lifetime of the photoinduced charge-transfer states is in the 1-10 µs range, depending on the sample and on temperature.

Introduction

The control by light of the physical and chemical properties (magnetic, optical, conductivity, motion, reactivity…) of materials is a challenging field of research from the fundamental and technological aspects. Optically switchable materials are extensively studied because of their potential applications in light-based technologies, such as optical memory devices or sensors for example. Several studies involving different kinds of materials have been reported, such as neutral-ionic or insulating-metal charge-transfer systems,[1] metal oxides,[2] photochromic materials,[3] spin-crossover complexes,[4] and cyanide-bridged bimetallic assemblies[5]. For these systems to be useful and in order to control their light-induced properties, it is compulsory to understand the elementary mechanisms that take place on the short time scale, allowing structural trapping of new electronic states. Molecule-based materials containing transition metal ions, such as Spin Crossover (SCO) systems and charge-transfer Prussian Blue Analogues (CT-PBA) possess a common behavior that is a very strong coupling between the electronic and structural changes after light illumination. The Light-Induced Excited Spin State Trapping (LIESST) phenomenon, was thoroughly investigated in many spin-crossover materials in the solid state[6]. Transient LIESST and its dynamics were studied by time-resolved techniques, including optical and X-ray spectroscopies, down to the femtosecond timescale, in solution[7] or in solids.[8] Ultrafast studies were also performed in cyanide-bridged bimetallic assemblies, using time-resolved optical,[9] Raman,[10] X-ray diffraction[11] and X-ray spectroscopy.[12] Optical and X-ray probe techniques are sensitive to both electronic and structural aspects and are therefore particularly interesting for understanding the transformation mechanisms of such materials.[8c] Here we use time-resolved X-ray Absorption Near Edge Structure (XANES) to evidence the transient charge transfer, induced by a laser pulse (~1 ps = 10^{-12} s), in two types of cyano-bridged photomagnetic networks in the form of nanocrystals for the compound noted CsCoFe and as powder for the compound noted RbMnFe in the following. The X-ray Absorption Near Edge Structure (XANES) experiments were performed at the ID09 beamline of the ESRF synchrotron and optical pump-probe studies were performed at the Institut de Physique de Rennes to characterize the lifetime of the transient CT states.

$Cs\{Co[Fe(CN)_6]\}$[5d] and $Rb\{Mn[Fe(CN)_6]\}$[5f] are photomagnetic materials known as Prussian Blue Analogues (PBA), consisting in face centered cubic (fcc) 3D network (Fig. 1(a)). The exact composition of the studied samples are given in experimental section and ESI. The CN^- groups bridge the two metal ions where Fe is linked to the carbon side of CN^- and Co and Mn to the nitrogen side. The alkali ions (Cs^I and Rb^I) occupy the tetrahedral sites of the fcc network. The metal ions have octahedral geometry with a symmetry very close to O_h. The octahedral crystal field of the ligands splits the 3d orbitals into two sets of t_{2g} and e_g orbitals. The Fe ions are always in the low spin (LS) state and the Mn ions in the high spin (HS) state. While the spin state of Co depends on its oxidation state; Co^{II} is high spin (S = 3/2) and Co^{III} is low spin (S = 0). For CsCoFe, there are, thus, two electronic configurations for the Co-Fe pairs i.e. the diamagnetic $Fe^{II}(S=0)$-$Co^{III}(S=0)$ and the paramagnetic $Fe^{III}(S=1/2)$-$Co^{II}(S=3/2)$. External control parameters like temperature or light allows switching between the two states as schematically represented by the potential energy curves in Fig. 1(b). At low temperature, light illumination allows an electron transfer from Fe^{II} to Co^{III} concomitant to a spin change to

[a] Serhane Zerdane, Lodovico Balducci, Marco Cammarata, Roman Bertoni, Eric Collet,
Univ Rennes 1, CNRS, Institut de Physique de Rennes, UMR 6251, UBL, F-35042 Rennes, France
E-mail: marco.cammarata@univ-rennes1.fr, eric.collet@univ-rennes1.fr
http://marcocamma.free.fr/ http://blogperso.univ-rennes1.fr/eric.collet/
[b] Laure Catala, Sandra Mazerat, Talal Mallah,
Univ Paris Sud, Université Paris-Saclay, CNRS, Institut de Chimie Moléculaire et des Matériaux d'Orsay, UMR 8182, Orsay, France.
[c] Martin N. Pedersen, Michael Wulff,
European Synchrotron Radiation Facility, F-38000 Grenoble, France.
[d] Kosuke Nakagawa, Shin-ichi Ohkoshi,
Department of Chemistry, School of Science, The University of Tokyo, 7-3-1 Hongo, Bunkyo-ku, Tokyo 113-0033, Japan.
[e] Hiroko Tokoro
Division of Materials Science, Faculty of Pure and Applied Sciences,

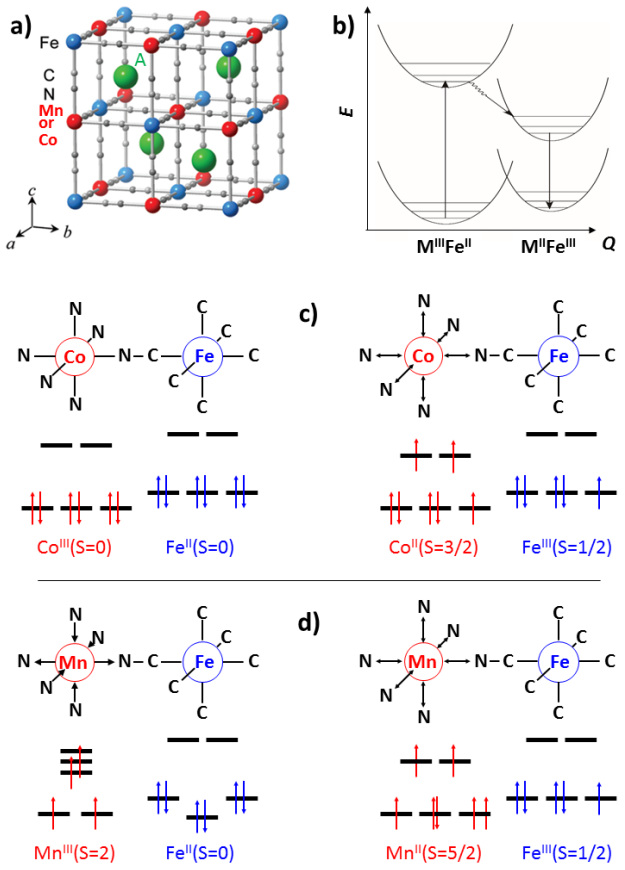

Figure 1. Schematic representation of the 3D structure (a) and potential energy curves (b) with electronic and structural changes associated with charge-transfer process in CsCoFe (c) and RbMnFe (d) systems.

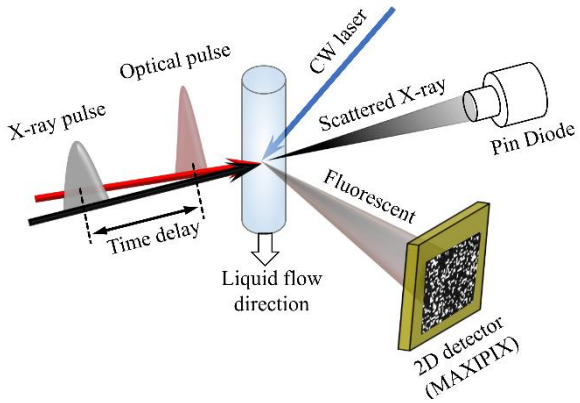

Figure 2. Schematic experimental set-up used for time-resolved XANES studies at the ESRF.

the higher entropy Fe^{III}(S=1/2)-Co^{II}(S=3/2) configuration. At thermal equilibrium, the change of spin state on the Co site is associated with a structural reorganization Fig. 1(c). As electron populates the antibonding e_g orbitals in the HS state, the Co-N bonds expand by about 0.2 Å, inducing a lattice expansion. Different alkali like Cs^I and Rb^I can be included in the tetrahedral sites of the fcc network to favor or not the higher volume state.

Bleuzen *et al.* demonstrated by XANES measurements at the Fe and Co edges that it is possible for a given composition of the material, to photoinduce the Co^{III}(LS)Fe^{II}(LS)→Co^{II}(HS)Fe^{III}(LS) charge transfer at room temperature under pressure.[5d]

For RbMnFe systems, there are also two possible electronic states: the ground one Mn^{III}(S=2)Fe^{II}(S=0), and the high-temperature one Mn^{II}(S=5/2)Fe^{III}(S=1/2) Fig. 1(d). The thermally-induced electron transfer was also characterized by XANES studies at the Fe and Mn edges, and here the main structural change occurs around the Mn site.[13] For both systems, the K edge XANES spectra are modified through their sensitivity to charge transfer (resulting in a “rigid shift” of the absorption spectra) and to structural rearrangement (change of the XANES spectrum). As detailed in the experimental section, we use these XANES fingerprints to track the electron transfer photoinduced by a femtosecond laser pulse, in CsCoFe and RbMnFe systems, by using the experimental set-up developed at the ID09 beamline of the ESRF (Figure 2). In addition, we use time-resolved optical spectroscopy to characterize the lifetime of the transient and out-of-equilibrium electron transfer.

Results and Discussion

The CsCoFe nanocrystals dispersed in water studied here are in the diamagnetic Fe^{II}(S=0)-Co^{III}(S=0) state at room temperature, which allows performing the photo transformation experiments at room temperature. We acquired the XANES data from the 15 nm size nanocrystals dispersed in water and excited by 650 nm laser pulses (Fig. 2). The XANES changes were monitored by the ≈70 ps X-ray pulses at the ID09 beamline as shown in Figure 3. Before laser irradiation, the maxima of X-ray absorption intensity I(a.u.) are around 7728 eV at the Co K-edge and around 7130 eV at the Fe K-edge. These results are in good agreement with the results obtained by Bleuzen *et al.*[5d] The spectral changes measured 500ps after laser excitation (red curve) are very weak. This is often the case in time-resolved studies, because the excitation density used is typically of the order of 1 photon per 100 active sites. Therefore, the spectral changes due to photoexcited species are better observed on the spectral intensity change, $\Delta I = (I_{500ps}-I_{off})$, also shown in Figure 3. The difference spectra at the Co edge shows a spectral shift towards lower energy, characterized by an absorption increase below the Co edge and a decrease just above. Difference spectra at Fe edge shows the opposite spectral shift towards higher energy, with an absorption decrease below the Fe edge and an increase just above.

Such changes in the absorption spectra are characteristic of the change of the formal oxidation state of the metal ions and therefore of the Co^{III}(LS)Fe^{II}→Co^{II}(HS)Fe^{III} electron transfer.[5d, 14] Additional oscillating changes above the Co edge are characteristic of the local structural change around Co due to the spin-crossover as already observed for Fe in the SCO systems.[7h] The transient XANES changes $\Delta I(t)$ after photoexcitation were measured at photon energies just above and below the Co and Fe absorption edges (Figure 4). These traces indicate that the electron transfer occurs within the 100 ps time resolution of the experiment and that the photoinduced Co^{II}(HS)Fe^{III} state has a lifetime larger than 1 ns at room temperature.

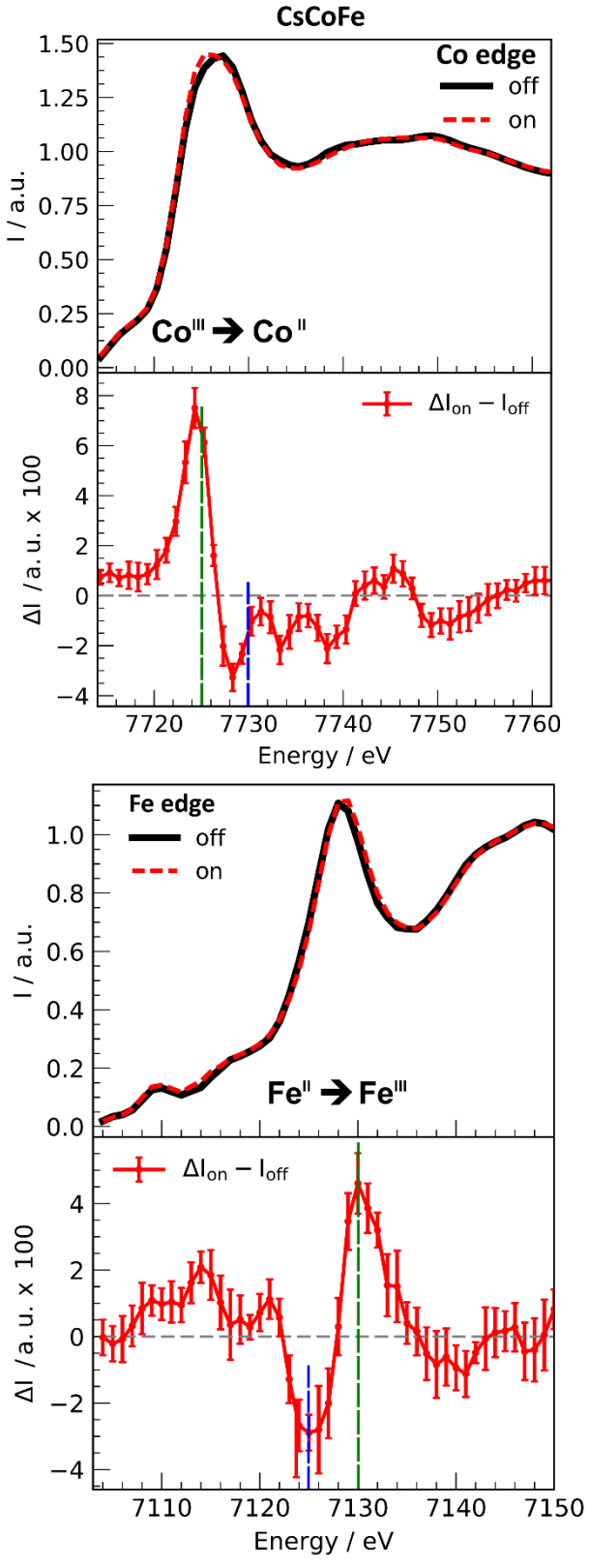

Figure 3. XANES spectra, for the CsCoFe nanocrystals, at the Fe and Co edges before (black) and 500 ps after laser excitation (red) and corresponding spectra change ΔI(t).

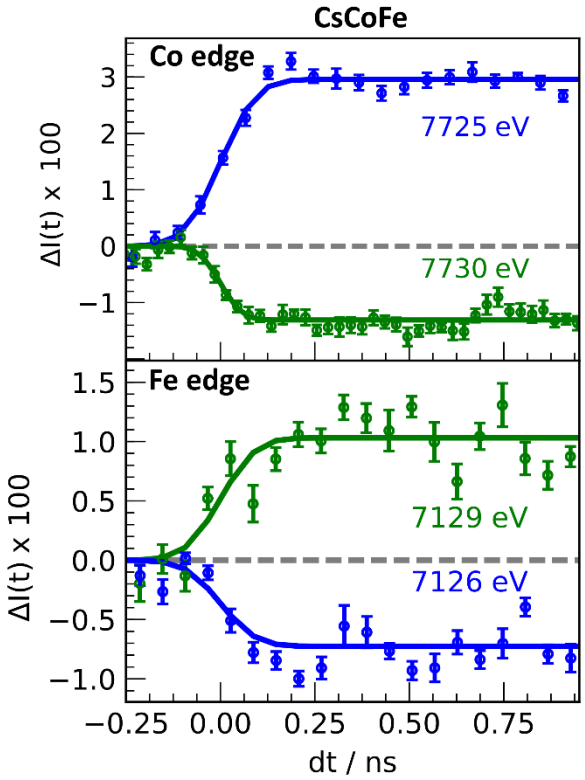

Figure 4. Time scans of relative absorption changes at selected X-ray energies below and above the Co and Fe edges, for he CsCoFe nanocrystals.

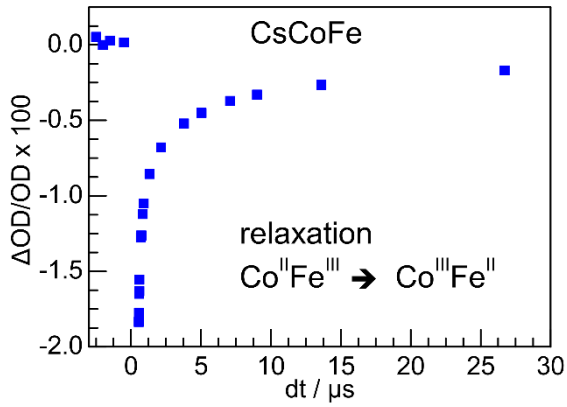

Figure 5. OD change at 520 nm, after fs laser at 650 nm, for he CsCoFe nanocrystals.

Cartier dit Moulin *et al* reported that the irradiation induces a shift for the preedge from 7711 to 7710 eV,[14a] hardly seen in Fig. 3 due to experimental limitations, which will be interesting to track in real time in future work.

For tracking the lifetime of the photoinduced Co^{II}(HS)Fe^{III}(LS) state, we performed complementary optical measurements on the experimental set-up available at the Institut de Physique de Rennes. We used time-resolved optical spectroscopy to study the relaxation process of CsCoFe nanocrystals in solution that were photo-excited at room temperature by 650 nm optical pulses.

The probe wavelength was set to 520 nm, which corresponds to the maximum of the $Co^{III}(LS)Fe^{II} \rightarrow Co^{II}(HS)Fe^{III}$ absorption band (Fig. S4). The time-resolved OD decrease after photoexcitation shown in Figure 5, is due to the depopulation of the $Co^{III}(LS)Fe^{II}$ after photoexcitation and indicates that the $Co^{II}(HS)Fe^{III} \rightarrow Co^{III}(LS)Fe^{II}$ relaxation occurs within few µs at room temperature.

We performed similar studies for the RbMnFe system. At the difference to the CsCoFe system, the RbMnFe is in the $Mn^{II}Fe^{III}$ state at room temperature. Upon cooling down, thermal electron transfer leads to the $Mn^{III}Fe^{II}$ state around 210 K with a complete conversion below 190 K. The thermal transition shows a thermal hysteresis and as the back conversion towards the $Mn^{II}Fe^{III}$ state occurs around 300 K.[5f] We measured the X-ray absorption at the Mn edge at room temperature (Figure 6). The maximum around 6551 eV is characteristic of the Mn^{II} state.[13] At lower temperature (210 K), the intensity of this peak decreases and a new one appears at 6557 eV characteristic of the Mn^{III} state and indicating the thermal conversion from Mn^{II} to Mn^{III}, as reported previously.[13] This temperature corresponds to the descending branch of the thermal hysteresis, where $Mn^{III}Fe^{II}$ and $Mn^{II}Fe^{III}$ states coexist. We observed additional changes of the spectrum change under cw laser excitation at 400 nm, which switches the system from $Mn^{II}Fe^{III}$ to $Mn^{III}Fe^{II}$ state.[5f] This is illustrated by the decrease (resp. increase) of the Mn^{II} (resp. Mn^{III}) peak in figure 6.

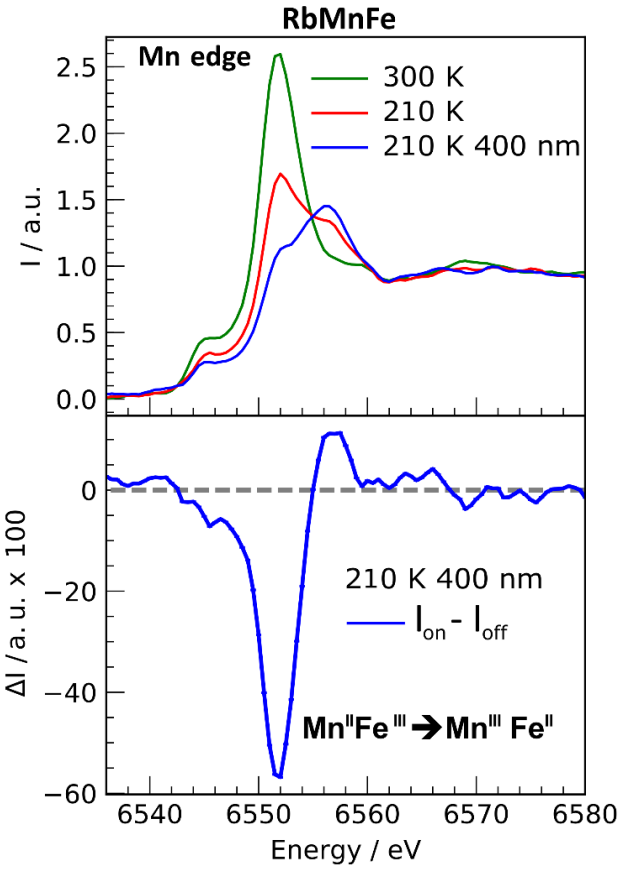

Figure 6. XANES spectra measured at the Mn edge, for the RbMnFe compound at room temperature, at 210 K and at 210 K under cw laser excitation at 400 nm, with corresponding spectral changes ΔI(t).

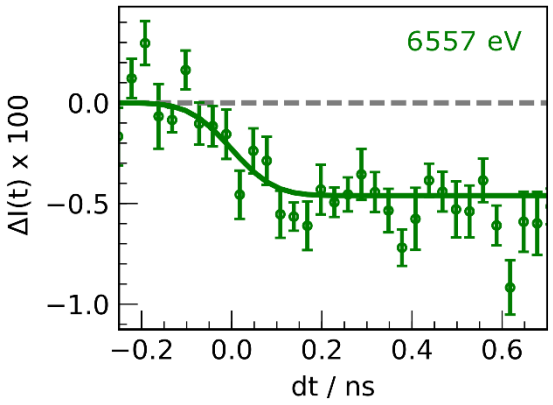

Figure 7. Time scans of relative absorption change 6557 eV for RbMnFe, after fs laser excitation at 530 nm.

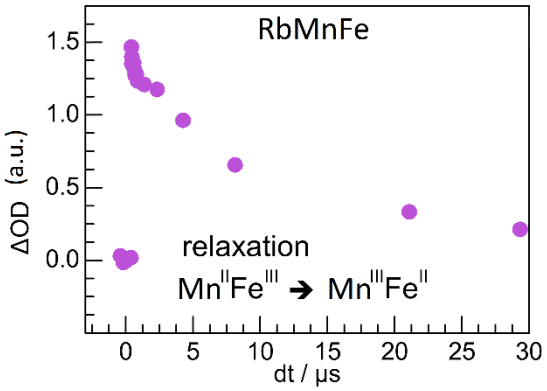

Figure 8. OD change, for he RbMnFe compound at 650 nm, after fs laser at 530 nm.

We then performed time-resolved XANES measurements on RbMnFe powder at 200 K. We monitored the transient XANES changes ΔI(t) at 6557 eV, induced by laser pulse photoexcitation at 530 nm, is known to induce the $Mn^{III}Fe^{II} \rightarrow Mn^{II}Fe^{III}$ electron transfer. The time trace reported in Figure 8 indicates that the electron transfer occurs within the ≈100 ps time resolution of the experiment. Time-resolved optical spectroscopy studies monitored the relaxation process of RbMnFe at 140 K, through the transient change of optical transmission intensity at 650 nm excitation by a fs laser pulse at 530 nm. The data presented in Figure 7 indicate that the $Mn^{II}Fe^{III} \rightarrow Mn^{III}Fe^{II}$ relaxation occurs within ≈10 µs.

Conclusions

The present study reveals transient CT state in different PBAs, characterized by time-resolved optical spectroscopy and time-resolved XANES. The lifetime of the CT states is in the 1-10 µs range in the 200-300 K range. This study also shows that it is possible to perform time-resolved studies with nano crystals in solution. It opens new possibilities to extend XANES studies at X-ray free electron laser, for tracking the intrinsic dynamics at sub-picosecond timescale, as recently performed for spin-crossover molecules in solution and in crystals.[7h, 8c, 8e, 8h]

Experimental Section

Synthesis and characterization of the $CsCoFe(CN)_6$ nanocrystals. The nanocrystals noted $CsCoFe(CN)_6$ were prepared by mixing two solutions one containing $K_3[Fe^{III}(CN)_6]$ and CsCl and one $Co^{II}Cl_2 \cdot 6H_2O$; they were recovered embedded in Polyvinylpyrrolidone (PVP) as already described for other similar nanocrystals.[15] The size of the objects was probed in solution before adding PVP and was found to be close to 15 nm (see ESI, Figure S1). The size was confirmed by Transmission Electron Microscopy imaging (see ESI, Figure S2). X-ray powder diffraction measurement gives the expected face centered cubic structure with a cell parameter of 9.96 Å characteristics of the Fe^{II}-Co^{III} lattice; an electron transfer from Co to Fe thus occurs during the nanocrystals' synthesis.[5d] The infra-red spectrum in the 2000-2200 cm^{-1} region has an intense band at 2112 nm corresponding to the asymmetric cyanide vibration of the Fe^{II}-CN-Co^{III} lattice; the weak band at 2070 corresponds to $Fe^{II}(CN)_6^{4-}$ species present at the surface of the 15 nm particles (see ESI, Figure S3). Elemental analysis gives the following composition $Cs_{0.58}\{Co[Fe(CN)_6]_{0.87}$. The time resolved XANES studies were performed on the nanocrystals embedded in PVP and dispersed in water. We also studied RbMnFe nanocrystals, obtained from a solution of manganese chlorides added to a mixed aqueous solution of rubidium chloride and potassium ferrocyanide. The precipitate is filtered and dried, giving a light brown powdered sample. By controlling the rubidium chloride concentration in the synthetic solution, samples with different compositions are realized. Elemental analyses of the prepared sample showed that the formula was $RbMn[Fe(CN)_6]_{0.96} \cdot 2.6H_2O$: Calculated; Rb, 21.64; Mn, 13.91; Fe, 13.86%: Found; Rb, 21.98; Mn, 13.85; Fe, 13.79%. A SEM photograph of this sample is provided in Fig. S5. Time-resolved optical pump-probe spectroscopy allowed tracking the lifetime of the charge-transfer states through optical absorption change. We used the optical pump-probe set-up described in ref[16], where the synchronization between the pump and probe femtosecond amplifiers is electronically tuned for 10 ns -ms delays, while a mechanical translation stage sets the optical path difference for sub-ns measurements. The experiments were configured in visible-NIR transmission geometry with a quasi-collinear configuration of pump and probe beams. We used 60 fs laser pulses at 650 nm (resp 532 nm) to photoexcite CsCoFe (resp. RbMnFe) and at 520 nm (resp. 650 nm) to probe the relaxation dynamics. More details about the experimental set-up are presented in the paper by Lorenc et al.[16]

The time resolved XANES measurements were performed using the optical pump / X-ray probe technique at the ID09 beamline. We used the X-ray pulses delivered from the ESRF using the 16 bunch-filling mode. The energy of X-ray emitted by the undulators (U27 and U17) was controlled by opening gap of the undulators. The X-ray beam passes through a cryo cooled (100K) Si(111) double crystal monochromator and is focused at the sample position with a toroidal mirror. Two choppers are used decrease the repetition rate of the X-ray train of pulses to 1kHz.[17] The temporal overlap of the X-ray/optic pulses is measured with the GaAs detector, which is sensitive to the both radiations, with a precision of 25 ps and the time delay between both pulses is electronically controlled. At the overlap position, the optical pump and the X-ray probe have respectively a pulse duration of 150 fs and 70 ps, with a focal area of 120 x 350 µm and 60 x 120 µm. The same was excited in quasi collinear geometry (angle between x-ray and laser beam of ~10°). The solution samples is circulated via a closed loop system through a 0.5 mm capillary tube and the rate flow is maintained using the peristaltic pump (Gilson Minipuls 3). The 2D detector (MAXIPIX) is mounted close to the sample (~ 3 cm) perpendicular to the X-ray propagation direction to minimize the collection of elastic photon scattering. In this geometry the active window (28.4 x 28.4 mm^2) covers a solid angle of ~ 0.74 sr (5.89 % of 4π). We used a Pin diode to measure simultaneously the transmission and scattered X-ray, in order to normalize the final fluorescence signal (Intensity fluctuation, the long decay of the current after each refill).

Acknowledgements

Parts of this research were carried out in the frame of the IM-LED LIA (CNRS) and a JSPS Grant-in-Aid for Specially promoted Research 15H05697 and JSPS KAKENHI 16H06521 Coordination Asymmetry. This work was supported by the ANR FEMTOMAT (ANR-13-BS04-0002) and from the European Union's Horizon 2020 Research and Innovation program under the Marie Skłodowska-Curie Grant Agreement No. 637295.

Keywords: Charge transfer • Magnetic properties • X-ray absorption spectroscopy • Time-resolved spectroscopy

References

[1] a) M. Gao, C. Lu, H. Jean-Ruel, L. C. Liu, A. Marx, K. Onda, S. Y. Koshihara, Y. Nakano, X. Shao, T. Hiramatsu, G. Saito, H. Yamochi, R. R. Cooney, G. Moriena, G. Sciaini, R. J. Miller, *Nature* **2013**, *496*, 343-346; b) S.-y. Koshihara, Y. Takahashi, H. Sakai, Y. Tokura, T. Luty, *The Journal of Physical Chemistry B* **1999**, *103*, 2592-2600; c) L. Guerin, J. Hebert, M. Buron-Le Cointe, S. Adachi, S. Koshihara, H. Cailleau, E. Collet, *Physical Review Letters* **2010**, *105*, -; d) E. Collet, M. Buron-Le Cointe, M. H. Lemée-Cailleau, H. Cailleau, L. Toupet, M. Meven, S. Mattauch, G. Heger, N. Karl, *Physical Review B* **2001**, *63*, 054105; e) E. Collet, M. H. Lemee-Cailleau, M. Buron-Le Cointe, H. Cailleau, M. Wulff, T. Luty, S. Y. Koshihara, M. Meyer, L. Toupet, P. Rabiller, S. Techert, *Science* **2003**, *300*, 612-615; f) T. Ishikawa, N. Fukazawa, Y. Matsubara, R. Nakajima, K. Onda, Y. Okimoto, S. Koshihara, M. Lorenc, E. Collet, M. Tamura, R. Kato, *Physical Review B* **2009**, *80*.

[2] a) M. Fiebig, K. Miyano, Y. Tomioka, Y. Tokura, *Journal of Applied Physics* **1999**, *85*, 5561-5563; b) S. Ohkoshi, Y. Tsunobuchi, T. Matsuda, K. Hashimoto, A. Namai, F. Hakoe, H. Tokoro, *Nat Chem* **2010**, *2*, 539-545; c) H. Tokoro, M. Yoshikiyo, K. Imoto, A. Namai, T. Nasu, K. Nakagawa, N. Ozaki, F. Hakoe, K. Tanaka, K. Chiba, R. Makiura, K. Prassides, S. Ohkoshi, *Nat Commun* **2015**, *6*, 7037.

[3] a) T. Fukaminato, T. Hirose, T. Doi, M. Hazama, K. Matsuda, M. Irie, *Journal of the American Chemical Society* **2014**, *136*, 17145-17154; b) M. Irie, T. Fukaminato, K. Matsuda, S. Kobatake, *Chemical Reviews* **2014**, *114*, 12174-12277.

[4] a) S. Decurtins, P. Gütlich, C. P. Köhler, H. Spiering, A. Hauser, *Chemical Physics Letters* **1984**, *105*, 1-4; b) A. Hauser, *Top Curr Chem* **2004**, *234*, 155-198; c) A. Goujon, F. Varret, K. Boukheddaden, C. Chong, J. Jeftić, Y. Garcia, A. D. Naik, J. C. Ameline, E. Collet, *Inorganica Chimica Acta* **2008**, *361*, 4055-4064; d) K. D. Murnaghan, C. Carbonera, L. Toupet, M. Griffin, M. M. Dirtu, C. Desplanches, Y. Garcia, E. Collet, J. F. Letard, G. G. Morgan, *Chemistry* **2014**, *20*, 5613-5618; e) J.-F. Létard, P. Guionneau, E. Codjovi, O. Lavastre, G. Bravic, D. Chasseau, O. Kahn, *Journal of the American Chemical Society* **1997**, *119*, 10861-10862; f) K. Ichiyanagi, J. Hebert, L. Toupet, H. Cailleau, P. Guionneau, J. F. Létard, E. Collet, *Physical Review B* **2006**, *73*; g) N. Brefuel, H. Watanabe, L. Toupet, J. Come, N. Matsumoto, E. Collet, K. Tanaka, J. P. Tuchagues, *Angew Chem Int Ed Engl* **2009**, *48*, 9304-9307; h) A. Bousseksou, G. Molnar, L. Salmon, W. Nicolazzi, *Chemical Society Reviews* **2011**, *40*, 3313-3335; i) E. Trzop, D. Zhang, L. Pineiro-Lopez, F. J. Valverde-Munoz, M. Carmen Munoz, L. Palatinus, L. Guerin, H. Cailleau, J. A. Real, E. Collet, *Angew Chem Int Ed Engl* **2016**, *55*, 8675-8679; j) J. E. Clements, J. R. Price, S. M. Neville, C. J. Kepert, *Angew Chem Int Ed Engl* **2016**, *55*, 15105-15109; k) E. Collet, M. L. Boillot, J. Hebert, N. Moisan, M. Servol, M. Lorenc, L. Toupet, M. Buron-Le Cointe, A. Tissot, J. Sainton, *Acta Crystallogr B* **2009**, *65*, 474-480.

[5] a) M. Verdaguer, A. Bleuzen, V. Marvaud, J. Vaissermann, M. Seuleiman, C. Desplanches, A. Scuiller, C. Train, R. Garde, G. Gelly, C. Lomenech, I. Rosenman, P. Veillet, C. Cartier, F. Villain, *Coordination Chemistry Reviews* **1999**, *190–192*, 1023-1047; b) R. Lescouezec, J. Vaissermann, C. Ruiz-Perez, F. Lloret, R. Carrasco, M. Julve, M. Verdaguer, Y. Dromzee, D. Gatteschi, W. Wernsdorfer, *Angewandte Chemie-International Edition* **2003**, *42*, 1483-1486; c) A. Dei, *Angewandte Chemie International Edition* **2005**, *44*, 1160-1163; d) J. D. Cafun, J. Lejeune, F. Baudelet, P. Dumas, J. P. Itie, A. Bleuzen, *Angew Chem Int Ed Engl* **2012**, *51*, 9146-9148; e) H. W. Liu, K. Matsuda, Z. Z. Gu, K. Takahashi, A. L. Cui, R. Nakajima, A. Fujishima, O. Sato, *Phys Rev Lett* **2003**, *90*, 167403; f) H. Tokoro, S. Ohkoshi, *Bulletin of the Chemical Society of Japan* **2015**, *88*, 227-239; g) K. Komori Orisaku, K. Nakabayashi, S. Ohkoshi, *Chem Lett* **2011**, *40*, 586-587; h) K. Zhang, S. Kang, Z. S. Yao, K. Nakamura, T. Yamamoto, Y. Einaga, N. Azuma, Y. Miyazaki, M. Nakano, S. Kanegawa, O. Sato, *Angew Chem Int Ed Engl* **2016**, *55*, 6047-6050; i) O. Sato, T. Iyoda, A. Fujishima, K. Hashimoto, *Science* **1996**, *272*, 704-705; j) F. Volatron, D. Heurtaux, L. Catala, C. Mathoniere, A. Gloter, O. Stephan, D. Repetto, M. Clemente-Leon, E. Coronado, T. Mallah, *Chem Commun* **2011**, *47*, 1985-1987; k) M. F. Dumont, E. S. Knowles, A. Guiet, D. M. Pajerowski, A. Gomez, S. W. Kycia, M. W. Meisel, D. R. Talham, *Inorganic Chemistry* **2011**, *50*, 4295-4300; l) S. Ohkoshi, S. Takano, K. Imoto, M. Yoshikiyo, A. Namai, H. Tokoro, *Nat Photon* **2014**, *8*, 65-71.

[6] M. A. Halcrow, *Spin-crossover materials : properties and applications*, Wiley, **2013**.

[7] a) G. Aubock, M. Chergui, *Nature Chemistry* **2015**, *7*, 629-633; b) W. K. Zhang, R. Alonso-Mori, U. Bergmann, C. Bressler, M. Chollet, A. Galler, W. Gawelda, R. G. Hadt, R. W. Hartsock, T. Kroll, K. S. Kjaer, K. Kubicek, H. T. Lemke, H. Y. W. Liang, D. A. Meyer, M. M. Nielsen, C. Purser, J. S. Robinson, E. I. Solomon, Z. Sun, D. Sokaras, T. B. van Driel, G. Vanko, T. C. Weng, D. L. Zhu, K. J. Gaffney, *Nature* **2014**, *509*, 345-348; c) J. K. McCusker, A. Vlček, *Accounts of Chemical Research* **2015**, *48*, 1207-1208; d) K. Hong, H. Cho, R. W. Schoenlein, T. K. Kim, N. Huse, *Accounts of Chemical Research* **2015**, *48*, 2957-2966; e) J. J. McGarvey, I. Lawthers, K. Heremans, H. Toftlund, *Journal of the Chemical Society, Chemical Communications* **1984**, 1575-1576; f) J. K. Mccusker, K. N. Walda, R. C. Dunn, J. D. Simon, D. Magde, D. N. Hendrickson, *Journal of the American Chemical Society* **1993**, *115*, 298-307; g) C. Bressler, C. Milne, V. T. Pham, A. ElNahhas, R. M. van der Veen, W. Gawelda, S. Johnson, P. Beaud, D. Grolimund, M. Kaiser, C. N. Borca, G. Ingold, R. Abela, M. Chergui, *Science* **2009**, *323*, 489-492; h) H. T. Lemke, K. S. Kjær, R. Hartsock, T. Brandt van Driel, M. Chollet, J. M. Glownia, S. Song, D. Zhu, E. Pace, S. F. Matar, M. N. Nielsen, M. Benfatto, K. J. Gaffney, E. Collet, M. Cammarata, *Nat. Commun.* **2017**, *8*, 15342; i) H. T. Lemke, C. Bressler, L. X. Chen, D. M. Fritz, K. J. Gaffney, A. Galler, W. Gawelda, K. Haldrup, R. W. Hartsock, H. Ihee, J. Kim, K. H. Kim, J. H. Lee, M. M. Nielsen, A. B. Stickrath, W. K. Zhang, D. L. Zhu, M. Cammarata, *Journal of Physical Chemistry A* **2013**, *117*, 735-740; j) W. K. Zhang, R. Alonso-Mori, U. Bergmann, C. Bressler, M. Chollet, A. Galler, W. Gawelda, R. G. Hadt, R. W. Hartsock, T. Kroll, K. S. Kjaer, K. Kubicek, H. T. Lemke, H. Y. W. Liang, D. A. Meyer, M. M. Nielsen, C. Purser, J. S. Robinson, E. I. Solomon, Z. Sun, D. Sokaras, T. B. van Driel, G. Vanko, T. C. Weng, D. L. Zhu, K. J. Gaffney, *Nature* **2014**, *509*, 345-348; k) S. E. Canton, X. Y. Zhang, L. M. L. Daku, A. L. Smeigh, J. X. Zhang, Y. Z. Liu, C. J. Wallentin, K. Attenkofer, G. Jennings, C. A. Kurtz, D. Gosztola, K. Warnmark, A. Hauser, V. Sundstrom, *Journal of Physical Chemistry C* **2014**, *118*, 4536-4545.

[8] a) R. Bertoni, M. Lorenc, H. Cailleau, A. Tissot, J. Laisney, M. L. Boillot, L. Stoleriu, A. Stancu, C. Enachescu, E. Collet, *Nat Mater* **2016**, *15*, 606-610; b) R. Bertoni, M. Lorenc, T. Graber, R. Henning, K. Moffat, J. F. Létard, E. Collet, *Crystengcomm* **2016**, *18*, 7269-7275; c) R. Bertoni, M. Cammarata, M. Lorenc, S. F. Matar, J. F. Letard, H. T. Lemke, E. Collet, *Acc Chem Res* **2015**, *48*, 774-781; d) R. Bertoni, M. Lorenc, A. Tissot, M. L. Boillot, E. Collet, *Coordination Chemistry Reviews* **2015**, *282-283*, 66-76; e) M. Cammarata, R. Bertoni, M. Lorenc, H. Cailleau, S. Di Matteo, C. Mauriac, S. F. Matar, H. Lemke, M. Chollet, S. Ravy, C. Laulhe, J. F. Letard, E. Collet, *Physical Review Letters* **2014**, *113*, 227402; f) R. Bertoni, M. Lorenc, A. Tissot, M. Servol, M. L. Boillot, E. Collet, *Angew Chem Int Ed Engl* **2012**, *51*, 7485-7489; g) E. Collet, N. Moisan, C. Balde, R. Bertoni, E. Trzop, C. Laulhe, M. Lorenc, M. Servol, H. Cailleau, A. Tissot, M. L. Boillot, T. Graber, R. Henning, P. Coppens, M. Buron-Le Cointe, *Phys Chem Chem Phys* **2012**, *14*, 6192-6199; h) A. Marino, M. Cammarata, S. F. Matar, J.-F. Létard, G. Chastanet, M. Chollet, J. M. Glownia, H. T. Lemke, E. Collet, *Structural Dynamics* **2016**, *3*, 023605; i) A. Marino, M. Buron-Le Cointe, M. Lorenc, L. Toupet, R. Henning, A. D. DiChiara, K. Moffat, N. Brefuel, E. Collet, *Faraday Discuss* **2015**, *177*, 363-379; j) A. Marino, P. Chakraborty, M. Servol, M. Lorenc, E. Collet, A. Hauser, *Angewandte Chemie-International Edition* **2014**, *53*, 3863-3867; k) S. Zerdane, L. Wilbraham, M. Cammarata, O. Iasco, E. Rivière, M. L. Boillot, I. Ciofini, E. Collet, *Chem. Sci.* **2017**.

[9] D. C. Arnett, P. Voehringer, N. F. Scherer, *Journal of the American Chemical Society* **1995**, *117*, 12262-12272.

[10] A. Asahara, M. Nakajima, R. Fukaya, H. Tokoro, S. Ohkoshi, T. Suemoto, *Physical Review B* **2012**, *86*.

[11] Y. Moritomo, T. Nakagawa, Y. Fukuyama, N. Yasuda, H. Oosawa, J. E. Kim, H. Kamioka, K. Kato, Y. Tanaka, S. Kimura, F. Nakada, S. Ohkoshi, H. Tanaka, M. Takata, *Journal of Physics: Conference Series* **2009**, *148*, 012028.

[12] Y. Moritomo, H. Kamioka, T. Shibata, S. Nozawa, T. Sato, S.-i. Adachi, *Journal of the Physical Society of Japan* **2013**, *82*, 033601.

[13] H. Osawa, T. Iwazumi, H. Tokoro, S. Ohkoshi, K. Hashimoto, H. Shoji, E. Hirai, T. Nakamura, S. Nanao, Y. Isozumi, *Solid State Communications* **2003**, *125*, 237-241.

[14] a) C. Cartier dit Moulin, F. Villain, A. Bleuzen, M.-A. Arrio, P. Sainctavit, C. Lomenech, V. Escax, F. Baudelet, E. Dartyge, J.-J. Gallet, M. Verdaguer, *Journal of the American Chemical Society* **2000**, *122*, 6653-6658; b) T. Yokoyama, Y. Murakami, M. Kiguchi, T. Komatsu, N. Kojima, *Physical Review B* **1998**, *58*, 14238-14244.

[15] a) D. Brinzei, L. Catala, N. Louvain, G. Rogez, O. Stephan, A. Gloter, T. Mallah, *Journal of Materials Chemistry* **2006**, *16*, 2593-2599; b) L. Catala, T. Mallah, *Coordination Chemistry Reviews* **2017**.

[16] M. Lorenc, C. Balde, W. Kaszub, A. Tissot, N. Moisan, M. Servol, M. Buron-Le Cointe, H. Cailleau, P. Chasle, P. Czarnecki, M. L. Boillot, E. Collet, *Physical Review B* **2012**, *85*.

[17] M. Cammarata, L. Eybert, F. Ewald, W. Reichenbach, M. Wulff, P. Anfinrud, F. Schotte, A. Plech, Q. Kong, M. Lorenc, B. Lindenau, J. Rabiger, S. Polachowski, *Rev Sci Instrum* **2009**, *80*, 015101.

Supporting Information

Probing transient photoinduced charge-transfer in Prussian Blue Analogues with time-resolved XANES and optical spectroscopy

S. Zerdane,[a] M. Cammarata,*[a] L. Balducci,[a] R. Bertoni,[a] L. Catala,[b] S. Mazerat, [b] T. Mallah, [b] M. N. Pedersen,[c] M. Wulff,[c] K. Nakagawa,[d] H. Tokoro,[e] S. Ohkoshi,[d] E. Collet,*[a]

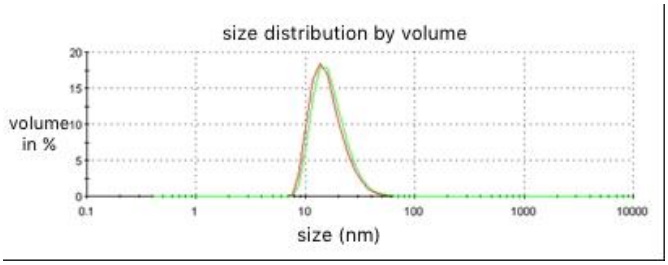

Figure S1. Dynamic Light Scattering measurement of CsCoFe nanocrystals in solution

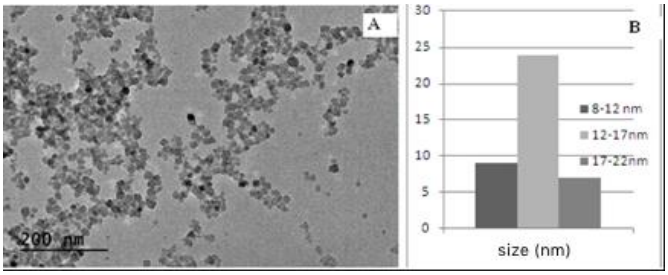

Figure S2. Transmission Electron Microscopy imaging of the CsCoFe nanocrystals (left) and size count (right).

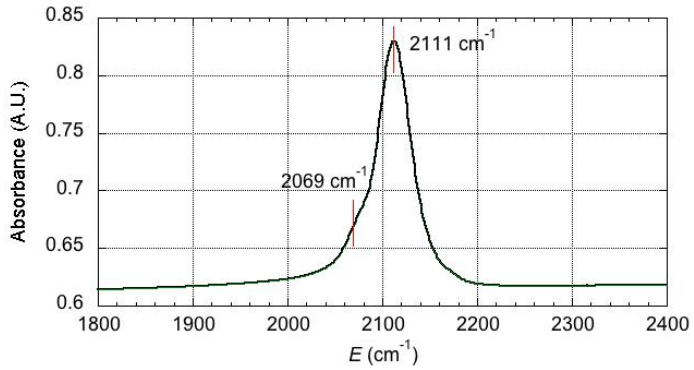

Figure S3. Infra-red spectrum of the CsCoFe nanocrystals embedded in PVP

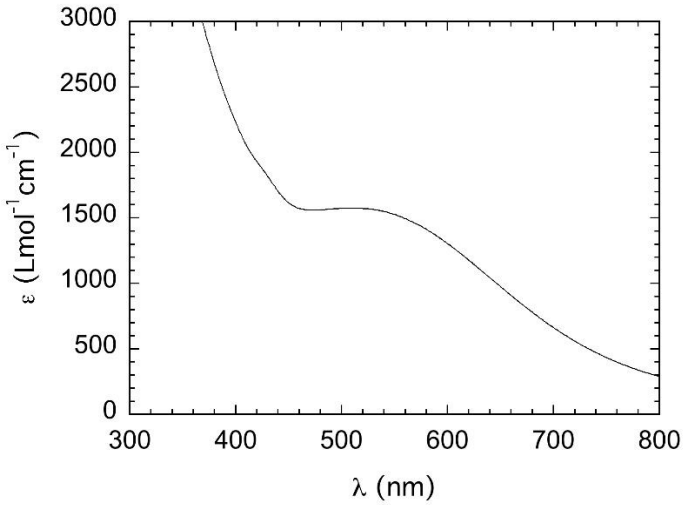

Figure S4. UV-vis spectrum of the CsCoFe nanocrystals in the $Co^{III}Fe^{II}$ state.

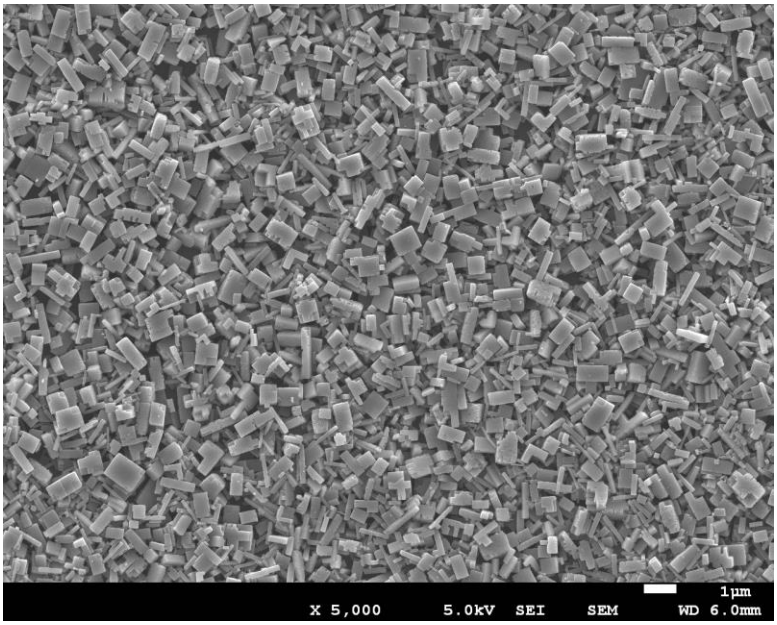

Figure S5. SEM photograph of the sample $RbMn^{II}[Fe^{III}(CN)_6]_{0.92}[Fe^{II}(CN)_6]_{0.06}\cdot 2.6H_2O$.